

18-DOF Triangular Quasi-Conforming Element for Couple Stress Theory

Xiangkui Zhang¹ and Changsheng Wang^{1,2} and Ping Hu¹

Abstract: The basic idea of quasi-conforming method is that the strain-displacement equations are weakened as well as the equilibrium equations. In this paper, an 18-DOF triangular element for couple stress theory is proposed within the framework of quasi-conforming technique. The formulation starts from truncated Taylor expansion of strains and appropriate interpolation functions are chosen to calculate strain integration. This element satisfies C^0 continuity with second order accuracy and weak C^1 continuity simultaneously. Numerical examples demonstrate that the proposed model can pass the C^{0-1} patch test and has high accuracy. The element does not exhibit extra zero energy modes and can capture the scale effects of microstructure.

Keywords: couple stress theory, triangular quasi-conforming element, enhanced patch test, scale effect

1 Introduction

The conventional elasticity theory assumes that a material is homogeneous throughout the region of interest, however, the theory does not account for the microstructures. In fact, all material consist of impurities, defects micro-cracks or crystal lattices, and the non-homogeneity in the microstructures and localization of deformation with respect to the failure state may lead to scale effects, such as the functionally-graded and laminated materials [Dong, El-Gizawy, Juhany, and Atluri (2014a,b)]. Numerous experiments conducted in the past several decades demonstrated strong scale effects when the material size scaling down to the order of micro-scale. For example, Fleck, Muller, Ashby, and Hutchinson (1994) discovered that the scaled shear strength increases by a factor of three as the wire diameter decreases from 170 to 12 μm in torsion experiments on copper wires. Simi-

¹ School of Automotive Engineering, State Key Laboratory of Structural Analysis for Industrial Equipment, Dalian University of Technology, Dalian 116024, P.R. China.

² changsheng@dlut.edu.cn

lar phenomena were observed in micro-indentation test [Nix and Gao (1998)] and micro-bend test [Wei, Wang, and Wu (2000)]. These experiments are commonly known as scale effects. Many theories have been developed for microstructures, such as the Cosserat theory, nonlocal elasticity theory, couple stress theory, and so on.

The couple stress/strain gradient elasticity is a phenomenological theory based on the methodology of continuum mechanics, which can explain the scale effect and localization of deformation. Couple stress theory can be seen as a special form of strain gradient theory. The difference of both theories is that the couple stress theory uses rotation as a variable to describe curvature, while the strain gradient theory uses strain to describe curvature. Both theories guarantee the connection with the conventional elasticity theory and take into account the microscopic properties of the material, thus can describe the localized deformation at micro-scale. In 1909 the bending moment was first introduced into the equilibrium equations by Cosserat brothers [Cosserat and Cosserat (1909)]. Then the theory was extended to a generalized elasticity theory by incorporating the strain gradient term into constitutive equations [Koiter (1964); Toupin (1962); Mindlin (1964)] and the couple stress theory was proposed. However, too many constitutive coefficients are included, which are difficult to determine. The strain gradient elasticity developed by Altan and Aifantis (1992) included only one material's characteristic length. The plastic strain gradient theories were derived by Aifantis (1984); Fleck and Hutchinson (1993, 1997). Yang, Chong, Lam, and Tong (2002) proposed symmetrical couple stress theory containing one material characteristic length constant.

Compared with the conventional elasticity theory, the couple stress theory is more complicated. Only first derivatives of displacements are contained in strain of conventional continuum 2D and 3D elasticity. However, the governing equations of couple stress/strain gradient theory contain the first and second derivatives of displacements simultaneously. Thus only a few analytical solutions are available, finite element method provides an alternative approach. However, the existing finite element programs are not able to deal with this type of problem, because that the elements based on couple stress theory should at least satisfy the requirement of C^1 continuity (continuous displacement and their derivatives). However, the complete C^1 continuous elements is difficult to construct due to too many parameters (including the displacements and their first and second derivatives) for one node. Up to now, only a few successful C^1 continuous conforming elements for higher-order theories have been proposed by researchers, such as Zervos, Papanastasiou, and Vardoulakis (2001); Zervos, Papanicolopoulos, and Vardoulakis (2009) and Papanicolopoulos, Zervos, and Vardoulakis (2009). However, such elements are inappropriate to apply in engineering for the difficult to apply boundary condition-

s due to higher order derivatives of node parameters. The C^1 continuity element with higher order derivatives of node parameters are rarely used even in the field of conventional continuum mechanics.

In order to obtain concise and high-accuracy couple stress elements, researchers resorted to nonconforming technique, and the patch test has been widely used for checking the convergence of nonconforming element. Soh and Chen (2004) proposed the C^{0-1} patch test (or enhanced patch test) for couple stress theory, they pointed out that the displacement functions for the C^{0-1} patch test should be quadratic polynomials and satisfy equilibrium equations without body force simultaneously. To pass the C^{0-1} patch test, the element displacement function must satisfy C^0 continuity and quadratic completeness. Researchers do lots of efforts to construct couple stress element: nodal parameters including displacement and their first order derivatives, C^1 continuity element, the second-order accuracy simultaneously and simple computation. The most commonly used method is using two types of element displacement functions: one satisfies C^0 continuity and quadratic completeness for calculating strains, and the other satisfies weak C^1 continuity for calculating strain gradients, such as Soh and Chen (2004); Zhao, Chen, and Lo (2011). Ma et al. adopted hybrid stress method to construct couple triangular and quadrilateral elements, Chen and Li (2014) applied B-net method to couple stress/strain gradient analysis.

The quasi-conforming technique was introduced by Tang, Chen, and Liu (1980) to meet the challenge of inter-elements conforming problems. Quasi-conforming finite element method is a very efficient theory framework, and its basic idea is the weakening of displacement-strain equations in the element together with that of the equilibrium equations. Similar to Pian's (1964) work on the assumed stress formulation, polynomials are used to describe the strain field, and the quasi-conforming method was called assumed strain method. Many elements are proposed during past few decades, the readers are refer to the review articles [Lombay, Suthasupradit, Kim, and Oñate (2009); Hu and Xia (2012)]. Hu, Xia, and Tang (2011) developed the assumed displacement quasi-conforming technique as a basic technique and constructed 4-node Reissner-Mindlin shell element. The assumed displacements quasi-conforming technique can give a simple and rational choice of initial strains which will be derived from the truncated Taylor expansion of displacements and the complicated process of rank analysis in assumed strain quasi-conforming technique can be avoided. Wang, Hu, and Xia (2012); Wang and Hu (2012) introduced a series of new interpolation functions and proposed new quadrilateral and triangular flat shell elements based on the assumed displacement quasi-conforming method.

In this paper, the quasi-conforming method was introduced to couple stress theory

analysis, and a 18-DOF triangular quasi-conforming element is proposed within the framework of quasi-conforming technique. The element can pass C^{0-1} patch test and has high accuracy, and it does not exhibit extra zero energy modes and can capture the scale effects of microstructure.

2 Plane couple stress theory

The couple stress theory contains second-order displacement gradients, and can be seen as the anti-symmetric case of strain gradient theory. The governing equations of the couple stress theory can be written as follows.

The geometric equation:

$$\boldsymbol{\varepsilon} = \begin{pmatrix} \varepsilon_x \\ \varepsilon_y \\ \gamma_s \end{pmatrix} = \begin{pmatrix} \frac{\partial u}{\partial x} \\ \frac{\partial v}{\partial y} \\ \frac{\partial u}{\partial y} + \frac{\partial v}{\partial x} \end{pmatrix} \tag{1}$$

$$\boldsymbol{\chi} = \begin{pmatrix} \chi_x \\ \chi_y \end{pmatrix} = \begin{pmatrix} \frac{\partial w}{\partial x} \\ \frac{\partial w}{\partial y} \end{pmatrix} = \begin{pmatrix} \frac{1}{2} \left(\frac{\partial^2 u}{\partial x \partial y} - \frac{\partial^2 v}{\partial^2 x} \right) \\ \frac{1}{2} \left(\frac{\partial^2 u}{\partial^2 y} - \frac{\partial^2 v}{\partial x \partial y} \right) \end{pmatrix}$$

in which $w = \frac{1}{2}(\partial u/\partial y - \partial v/\partial x)$. ε_x , ε_y and γ_s are normal and shear strains in continuum mechanics, and χ_x , χ_y are curvatures in micro-scale.

The constitutive equation:

$$\boldsymbol{\sigma} = \begin{pmatrix} \sigma_x \\ \sigma_y \\ \tau_s \end{pmatrix} = \mathbf{D}_a \begin{pmatrix} \varepsilon_x \\ \varepsilon_y \\ \gamma_s \end{pmatrix} \tag{2}$$

$$\mathbf{m} = \begin{pmatrix} m_x \\ m_y \end{pmatrix} = \mathbf{D}_c \begin{pmatrix} \chi_x \\ \chi_y \end{pmatrix}$$

$$\mathbf{D}_a = \begin{pmatrix} D_1 & \frac{\mu D_1}{1-\mu} \\ \frac{\mu D_1}{1-\mu} & D_1 \end{pmatrix} \quad \mathbf{D}_c = \begin{pmatrix} 4l^2 G & \\ & 4l^2 G \end{pmatrix} \tag{3}$$

where σ_x , σ_y , τ_s are normal and shear stresses in continuum mechanics, m_x , m_y bending momentums in micro-scale. E , μ are constants of elasticity, while $D_1 =$

$E(1 - \mu)/((1 + \mu)(1 - 2\mu))$, $G = E/(2(1 + \mu))$. l is the material characteristic length constant at the micro-scale, which describes the constitutive relations of the material on the microscopic scale. Bažant (2002); Bažant and Pang (2007) gives the method to determined l for different kinds of materials. The conventional continuum theory is recovered when the characteristic length of the material l approaches infinitesimal.

The equilibrium equation(without body forces):

$$\begin{cases} \frac{\partial \sigma_x}{\partial x} + \frac{\partial \tau_s}{\partial y} - \frac{1}{2} \left(\frac{\partial^2 m_x}{\partial x \partial y} + \frac{\partial^2 m_y}{\partial^2 y} \right) = 0 \\ \frac{\partial \sigma_y}{\partial y} + \frac{\partial \tau_s}{\partial x} - \frac{1}{2} \left(\frac{\partial^2 m_x}{\partial^2 x} + \frac{\partial^2 m_y}{\partial x \partial y} \right) = 0 \end{cases} \quad (4)$$

The boundary forces:

$$\mathbf{T} = \begin{pmatrix} T_{mx} \\ T_{my} \\ T_w \end{pmatrix} = \begin{pmatrix} \sigma_x n_x + \tau_s n_y - \frac{1}{2} \left(\frac{\partial m_x}{\partial x} + \frac{\partial m_y}{\partial y} \right) n_y \\ \sigma_y n_y + \tau_s n_x - \frac{1}{2} \left(\frac{\partial m_x}{\partial x} + \frac{\partial m_y}{\partial y} \right) n_x \\ m_x n_x + m_y n_y \end{pmatrix} \quad (5)$$

Substituting equations (1) and (2) into (4), the couple stress equilibrium equation in terms of displacements (without body force) can be obtained

$$\begin{cases} \frac{E}{(1 + \mu)(1 - 2\mu)} \left((1 - \mu) \frac{\partial^2 u}{\partial x^2} + \frac{(1 - 2\mu)}{2} \frac{\partial^2 u}{\partial y^2} + \frac{1}{2} \frac{\partial^2 v}{\partial x \partial y} \right) \\ - l^2 G \left(\frac{\partial^4 u}{\partial x^2 \partial y^2} - \frac{\partial^4 v}{\partial x^3 \partial y} + \frac{\partial^4 u}{\partial y^4} - \frac{\partial^4 v}{\partial x \partial y^3} \right) = 0 \\ \frac{E}{(1 + \mu)(1 - 2\mu)} \left(\frac{(1 - 2\mu)}{2} \frac{\partial^2 v}{\partial x^2} + (1 - \mu) \frac{\partial^2 v}{\partial y^2} + \frac{1}{2} \frac{\partial^2 u}{\partial x \partial y} \right) \\ - l^2 G \left(\frac{\partial^4 u}{\partial x^3 \partial y} - \frac{\partial^4 v}{\partial x^4} + \frac{\partial^4 u}{\partial x \partial y^3} - \frac{\partial^4 v}{\partial x^2 \partial y^2} \right) = 0 \end{cases} \quad (6)$$

In C^{0-1} patch test, the test function should satisfy the equilibrium equation (6) in the form of displacements.

3 Formulation of 18-DOF quasi-conforming element based on couple stress theory

3.1 Formulation of quasi-conforming element

In the quasi-conforming technique, the element strain fields are approximated using polynomials and integrated using interpolation functions. The strain $\boldsymbol{\varepsilon}$ can be

approximated as

$$\boldsymbol{\varepsilon} = \mathbf{Q}\boldsymbol{\alpha} \tag{7}$$

where \mathbf{Q} is strain interpolation polynomial function matrix, and $\boldsymbol{\alpha}$ is undetermined strain parameter vector.

Letting \mathbf{W} be the test function, then equation (7) can be rewritten into the weak form

$$\int_{\Omega} \mathbf{W}(\boldsymbol{\varepsilon} - \mathbf{Q}\boldsymbol{\alpha})d\Omega = 0 \tag{8}$$

where Ω represents the element domain. Generally, the test function is taken as $\mathbf{W} = \mathbf{Q}^T$, then $\boldsymbol{\alpha}$ can be determined by carrying out the integration:

$$\boldsymbol{\alpha} = \mathbf{A}^{-1}\mathbf{C}\mathbf{q} \tag{9}$$

in which

$$\mathbf{A} = \int_{\Omega} \mathbf{Q}^T\mathbf{Q}d\Omega \tag{10}$$

$$\mathbf{C}\mathbf{q} = \int_{\Omega} \mathbf{Q}^T\boldsymbol{\varepsilon}d\Omega \tag{11}$$

where \mathbf{q} is element nodal displacement vector.

Substituting $\boldsymbol{\alpha}$ in equation (9) into (7) defines the strains in terms of the element nodal displacements

$$\boldsymbol{\varepsilon} = \mathbf{Q}\boldsymbol{\alpha} = \mathbf{Q}\mathbf{A}^{-1}\mathbf{C}\mathbf{q} = \mathbf{B}\mathbf{q} \tag{12}$$

Then the element stiffness matrix can be easily obtained

$$\mathbf{K} = \int_{\Omega} \mathbf{B}^T\mathbf{D}\mathbf{B}d\Omega = \mathbf{C}^T\mathbf{A}^{-T} \int_{\Omega} \mathbf{Q}^T\mathbf{D}\mathbf{Q}d\Omega\mathbf{A}^{-1}\mathbf{C} \tag{13}$$

in which \mathbf{D} is the elasticity matrix.

The number of terms of initial assumed strain in equation (7) should meet the rank analysis. A general approach for the rank analysis of the quasi-conforming technique was given in [Liu, Shi, and Tang (1983)].

The integrals in equation (11) can be evaluated by using Green's theorem. Assumed $H^1(\Omega)$ is Hilbert space, Ω is the element field, V_{Ω} is a finite dimensional subspace of $H^1(\Omega)$, $u_{,x} \in V_{\Omega}$ is the approximation of derivative $\partial u/\partial x$. The derivative relations can be weakened within the field of the element by using Green's theorem

$$\int_{\Omega} wu_{,x}d\Omega = \oint_S wun_x ds - \int_{\Omega} \frac{\partial w}{\partial x}ud\Omega \quad \forall w \in V_{\Omega} \tag{14}$$

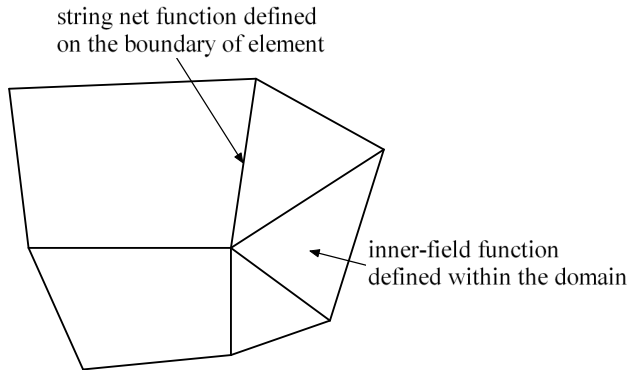


Figure 1: Multiple function set for an element.

There are two functions $u|_{\Omega}$ and $u|_{\partial\Omega}$ in the right side of the formulation, as shown in Fig 1. Since $u_{,x}$ is a approximation of derivative $\partial u/\partial x$, then $u|_{\Omega}$ and $u|_{\partial\Omega}$ can be replaced by function u_{Ω} within the element field and u_b on the boundary of the element respectively, while u_b may not equal to $u_{\Omega}|_{\partial\Omega}$ [Shi and Wang (2013)]. Then the equation can be rewritten as

$$\int_{\Omega} w u_{,x} d\Omega = \oint_S w u_b n_x ds - \int_{\Omega} \frac{\partial w}{\partial x} u_{\Omega} d\Omega \quad \forall w \in V_{\Omega} \tag{15}$$

It is worth pointing out that u_b can not be the restriction of u_{Ω} on the boundary of the element. A important task when constructing the quasi-conforming element is to ensure the continuity of finite element function when across the inner-boundary of elements, meanwhile the string net function on the boundary can be irrelevant with the inner-field function. However, if the inner-field function which degraded to boundary is equal to the string net function, then we get conforming element, otherwise, we get nonconforming element.

3.2 Formulation of 18-DOF couple stress quasi-conforming element

Based on the plane couple stress theory and quasi-conforming method, the formulation of 18-DOF couple stress element is proposed below, and each node has six degrees of freedom, as shown in Fig 2. The element stiffness matrix can be divided into two parts:

$$\mathbf{K} = \mathbf{K}_a + \mathbf{K}_c \tag{16}$$

$$\mathbf{K}_a = \iint_{\Omega} \boldsymbol{\epsilon}^T \mathbf{D}_a \boldsymbol{\epsilon} dx dy \tag{17}$$

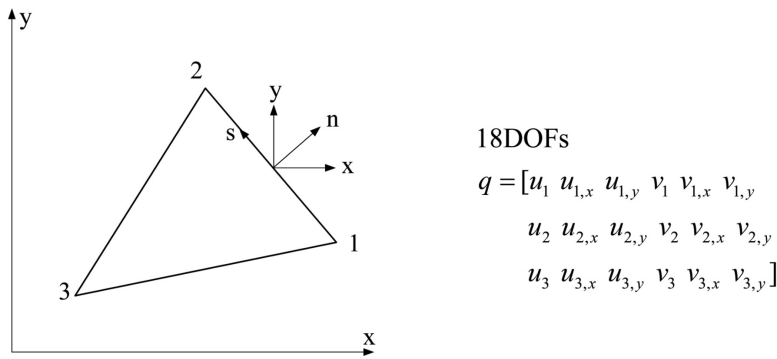


Figure 2: Model of triangular quasi-conforming element.

$$\mathbf{K}_c = \iint_{\Omega} \boldsymbol{\chi}^T \mathbf{D}_c \boldsymbol{\chi} dx dy \tag{18}$$

in which \mathbf{K}_a is the element stiffness of strain part, \mathbf{K}_c the element stiffness of strain gradient part, Ω the field of the element, other parameters defined in equations (1) and (3). By using the equations (13) of section 3.2, we can get the stiffness matrix of the element.

The strain $\boldsymbol{\varepsilon}$ in equation (1) can be approximated by using the following initial displacement assumption

$$\begin{cases} u = a_1 + a_2x + a_3y + a_4x^2 + a_5xy + a_6y^2 + a_7x^2y + a_8xy^2 \\ v = b_1 + b_2x + b_3y + b_4x^2 + b_5xy + b_6y^2 + b_7x^2y + b_8xy^2 \end{cases} \tag{19}$$

in which a_i and b_i ($i = 1 \dots 8$) are the unknown parameters of displacements. Substituted (19) into (1) we can get the initial strain approximation, denoted as

$$\boldsymbol{\varepsilon} = \mathbf{P}_a \boldsymbol{\alpha}_a \tag{20}$$

Then $\boldsymbol{\alpha}_a$ can be evaluated as follows

$$\begin{aligned} \boldsymbol{\alpha}_a &= \mathbf{A}_a^{-1} \mathbf{C}_a \mathbf{q} \\ \mathbf{A}_a &= \iint_{\Omega} \mathbf{P}_a^T \mathbf{P}_a dx dy \\ \mathbf{C}_a \mathbf{q} &= \iint_{\Omega} \mathbf{P}_a^T \boldsymbol{\varepsilon} dx dy \end{aligned} \tag{21}$$

Matrix \mathbf{A}_a involves the integrals of polynomials which can be carried out quite easily, and the essential work is the evaluation of matrix \mathbf{C}_a . The Green's theorem

should be used, taking the derivative $\partial u/\partial x$ as example.

$$\begin{aligned}\iint_{\Omega} \frac{\partial u}{\partial x} dx dy &= \oint_s u n_x ds \\ \iint_{\Omega} \frac{\partial u}{\partial x} x dx dy &= \oint_s u n_x x ds - \iint_{\Omega} u dx dy \\ \iint_{\Omega} \frac{\partial u}{\partial x} y dx dy &= \oint_s u n_x y ds\end{aligned}\quad (22)$$

For the boundary integration, the following transformation equations are needed

$$\begin{pmatrix} u_x \\ u_y \end{pmatrix} = \begin{pmatrix} n_x & -n_y \\ n_y & n_x \end{pmatrix} \begin{pmatrix} u_s \\ u_n \end{pmatrix}\quad (23)$$

in which $n_x = \cos(\mathbf{n}, \mathbf{x})$, $n_y = \cos(\mathbf{n}, \mathbf{y})$. Take u of boundary 1 – 2 as an example, the string net function can be chosen as

$$\begin{cases} u = N_1 u_1 + N_2 u_{1,s} + N_3 u_2 + N_4 u_{2,s} \\ u_{,n} = L_1 u_{1,n} + L_2 u_{2,n} \\ u_{,s} = -(6L_1 L_2 / L) u_1 + L_1 (1 - 3L_2) u_{1,s} + -(6L_1 L_2 / L) u_2 + L_2 (1 - 3L_1) u_{2,s} \end{cases}\quad (24)$$

in which L is the length of boundary 1 – 2, $L_1 = 1 - s/L$, $L_2 = s/L$, s is the coordinate along the boundary. NS_1, NS_2, NS_3, NS_4 are shape functions

$$\begin{cases} NS_1 = L_1 + L_1 L_2 (L_1 - L_2) \\ NS_2 = (L_1 L_2 + L_1 L_2 (L_1 - L_2)) L / 2 \\ NS_3 = L_2 + L_1 L_2 (L_2 - L_1) \\ NS_4 = (-L_1 L_2 + L_1 L_2 (L_1 - L_2)) L / 2 \end{cases}\quad (25)$$

Besides, the integral $\iint_{\Omega} u dx dy$, $\iint_{\Omega} u x dx dy$ and $\iint_{\Omega} u y dx dy$ should be calculated. u can be chosen as the displacement function CT9 in Soh and Chen (2004)

$$u = \bar{\mathbf{N}} \mathbf{q}^u\quad (26)$$

$$\begin{cases} \bar{\mathbf{N}} = [\bar{\mathbf{N}}_1, \bar{\mathbf{N}}_2, \bar{\mathbf{N}}_3] \\ \bar{\mathbf{N}}_j = [R_j, R_{xj}, R_{yj}] \quad (j = 1, 2, 3) \\ \mathbf{q}^u = \left(u_1 \quad u_{1,x} \quad u_{1,y} \quad u_2 \quad u_{2,x} \quad u_{2,y} \quad u_3 \quad u_{3,x} \quad u_{3,y} \right)^T \end{cases}\quad (27)$$

$$\begin{cases} R_1 = 0.5(-n_{x1} N_4 / S_1 + N_{x3} N_6 / S_3) + F_1 \\ R_{x1} = -0.125(n_{x1}^2 N_4 + n_{x3}^2 N_6) \\ R_{y1} = 0.125(n_{x1} n_{y1} N_4 + n_{x3} n_{y3} N_6) \end{cases}\quad (28)$$

where N_i ($i = 1 \dots 6$) are the shape functions of the 6-node triangular element in terms of area co-ordinates (F_i ($i = 1, 2, 3$)). Other shape functions \bar{N}_j ($j = 2, 3$) can be obtained by cyclic permutation. x, y as follows

$$\begin{aligned} x &= F_1x_1 + F_2x_2 + F_3x_3 \\ y &= F_1y_1 + F_2y_2 + F_3y_3 \end{aligned} \tag{29}$$

Thus the element stiffness matrix of strain part can be denoted as by using equations (17) (20) and (21)

$$\mathbf{K}_a = \iint_{\Omega} \boldsymbol{\epsilon}^T \mathbf{D}_a \boldsymbol{\epsilon} dxdy = \mathbf{C}_a^T \mathbf{A}_a^{-T} \int_{\Omega} \mathbf{P}_a^T \mathbf{D}_a \mathbf{P}_a dxdy \mathbf{A}_a^{-1} \mathbf{C}_a \tag{30}$$

The strain gradient $\boldsymbol{\chi}$ in equation (1) can be approximated directly as

$$\begin{aligned} \boldsymbol{\chi} &= \mathbf{P}_c \boldsymbol{\alpha}_c \\ \mathbf{P}_c &= \begin{pmatrix} 1 & x & y & 0 & 0 & 0 \\ 0 & 0 & 0 & 1 & x & y \end{pmatrix} \end{aligned} \tag{31}$$

Like the strain part, the element stiffness matrix of strain gradient part can be denoted as

$$\mathbf{K}_c = \iint_{\Omega} \boldsymbol{\chi}^T \mathbf{D}_c \boldsymbol{\chi} dxdy = \mathbf{C}_c^T \mathbf{A}_c^{-T} \int_{\Omega} \mathbf{P}_c^T \mathbf{D}_c \mathbf{P}_c dxdy \mathbf{A}_c^{-1} \mathbf{C}_c \tag{32}$$

where

$$\begin{aligned} \mathbf{A}_c &= \iint_{\Omega} \mathbf{P}_c^T \mathbf{P}_c dxdy \\ \mathbf{C}_c \mathbf{q} &= \iint_{\Omega} \mathbf{P}_c^T \boldsymbol{\chi} dxdy \end{aligned} \tag{33}$$

By using the Green's theorem in Appendix A, only string-net functions are used to calculate strain gradient integration and the string-net functions are chosen as in equation (24). Then the element stiffness \mathbf{K}_c of the strain gradient can be derived by using equation (13).

4 Numerical examples

In this section, several existing appropriate examples are used to evaluate the performance of the new element.

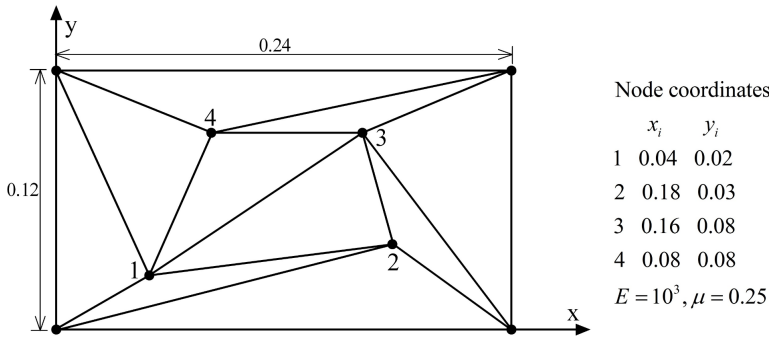


Figure 3: Mesh for patch test.

4.1 C^{0-1} patch test

Different from constant curvature patch test, the displacement functions of C^{0-1} patch test should be a quadratic polynomial to satisfy the equilibrium equations inside the element. The test displacement functions can be assumed as follows based on the C^{0-1} patch test proposed by Soh and Chen (2004):

$$\begin{cases} u = a_1 + a_2x + a_3y + a_4x^2 + a_5xy + a_6y^2 \\ v = b_1 + b_2x + b_3y + b_4x^2 + b_5xy + b_6y^2 \end{cases} \quad (34)$$

in which a_i, b_i ($i = 1 \dots 6$) are constants to be determined. Substituting equations (34) into equilibrium equations (6), the test displacement functions of couple stress element can be obtained as follows:

$$\begin{cases} u = a_1 + a_2x + a_3y + a_4x^2 - 2[(1 - 2\mu)b_4 + 2(1 - \mu)b_6]xy + a_6y^2 \\ v = b_1 + b_2x + b_3y + b_4x^2 - 2[2(1 - \mu)a_4 + (1 - 2\mu)a_6]xy + b_6y^2 \end{cases} \quad (35)$$

then the rotation displacement functions $u_{,x}, u_{,y}, v_{,x}, v_{,y}$ can be calculated by:

$$\begin{cases} u_{,x} = \frac{\partial u}{\partial x} = a_2 + 2a_4x - 2((1 - 2\mu)b_4 + 2(1 - \mu)b_6)y \\ u_{,y} = \frac{\partial u}{\partial y} = a_3 - 2((1 - 2\mu)b_4 + 2(1 - \mu)b_6)x + 2a_6y \\ v_{,x} = \frac{\partial v}{\partial x} = b_2 + 2b_4x - 2((1 - 2\mu)a_4 + 2(1 - \mu)a_6)y \\ v_{,y} = \frac{\partial v}{\partial y} = b_3 - 2((1 - 2\mu)a_4 + 2(1 - \mu)a_6)x + 2b_6y \end{cases} \quad (36)$$

The mesh model for patch test is shown in Fig. 3, and the coefficients a_i and b_i of the test functions in equations (34) are listed in Table 1. The material parameters are

$l = 0.5, E = 1000$ and $\mu = 0.25$. The boundary displacements can be determined by equations (34), which are imposed as the displacement boundary conditions.

The numerical results of the patch are listed in Table 2. These results demonstrate that the quasi-conforming element can pass the C^{0-1} patch test.

Table 1: The coefficients of C^{0-1} patch test functions.

a_1	a_2	a_3	a_4	a_5	b_1	b_2	b_3	b_4	b_5
1	3	5	7	9	2	4	6	8	10

Table 2: Numerical results of C^{0-1} patch test.

	u_1	$\partial u_1 / \partial x$	$\partial u_1 / \partial y$	v_1	$\partial v_1 / \partial x$	$\partial v_1 / \partial y$
Quasi-conforming element	1.2044	2.8000	3.8400	2.2728	4.0400	5.2000
Exact solution	1.2044	2.8000	3.8400	2.2728	4.0400	5.2000

4.2 Eigenvalue test

The eigenvalue test is adopted here to test if the element is free from the spurious zero energy modes. A typical triangular element shown in Fig. 4 is used in the test: height = 10, width = 10, thickness = 1.0, and the material parameters $E = 1000, \mu = 0.25, l = 0.1$. The number of spurious zero energy modes equal to the number of zero eigenvalue minus the number of rigid body motions. Three

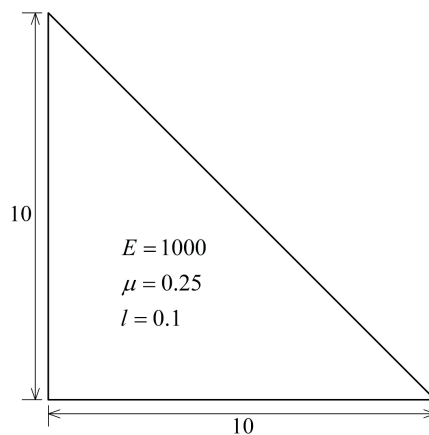


Figure 4: Typical element for the eigenvalue test.

triangular elements that satisfy the C^{0-1} patch test in Soh and Chen (2004) are also selected to compare with the proposed quasi-conforming element, they are:

- (i) BCIZ+RT9: non-conforming element BCIZ for calculating strains and element RT9 for strain gradients;
- (ii) CT9+RT9: element CT9 for calculating strains and element RT9 for strain gradients;
- (iii) RCT9+RT9: element RCT9 for calculating strains and element RT9 for strain gradients;

The results are listed in Table 3. It is worth noting that among the elements that satisfy the C^{0-1} patch test, the element CT9+RT9 has spurious zero energy mode, whereas the quasi-conforming element is free from zero energy mode.

Table 3: The coefficients of enhanced patch test functions.

Element	BCIZ+RT9	CT9+RT9	RCT9+RT9	Quasi-conforming element
Eigenvalue	3.19045E-13	-2.82322E-14	-7.75867E-14	1.17830E-13
	8.80575E-13	-1.60301E-13	-3.53450E-14	3.71996E-13
	-2.75611E-13	-5.65891E-13	2.93807E-13	-4.1870E-13
		5.02404E-13		
	(5.14034E+01)	(1.40553E-01)	(1.86189E+01)	(4.48338E+02)
Spurious zero modes	3 - 3 = 0	4 - 3 = 1	3 - 3 = 0	3 - 3 = 0

4.3 Pure bending problem

In this section, the bending beam model subjected to a moment in the right hand is shown in Fig. 5, which is same as those in Stölken's micro bending test [Stölken and Evans (1998)]. The length of beam $L = 250 \mu\text{m}$, depth of beam $h = 12.5 \mu\text{m}$, the elastic modulus $E = 220 \text{ GPa}$, the Poisson's ratio $\mu = 0.31$, the bending moment $M = 50 \text{ N}\mu\text{m}$. The analytical solution by the couple stress theory is given as [Ji and Chen (2010)]:

$$v = -\frac{6M(1-\mu^2)}{Eh(h^2 + 24(1-\mu)l^2)} \left(x^2 + \frac{\mu}{1-\mu} y^2 \right) \quad (37)$$

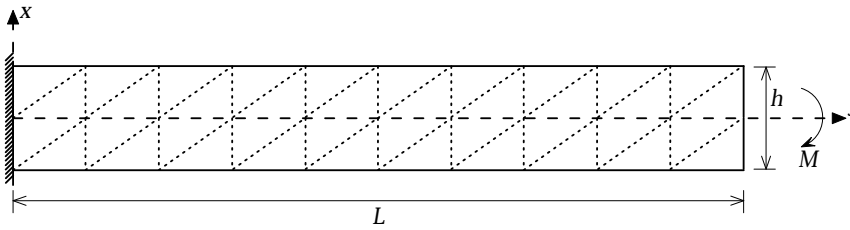


Figure 5: Mesh model of pure bending beam (10×2).

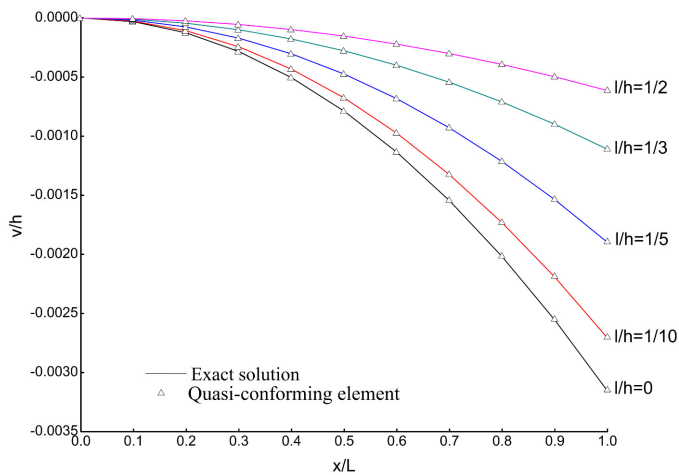


Figure 6: The deflection of pure bending for various ratios l/h (10×2).

Numerical analysis is done with uniform 10×2 mesh (Fig. 5) by using quasi-conforming triangular element. Keep the beam constant and change the material constant $l/h = \{0, 1/10, 1/5, 1/3, 1/2\}$ to examine the scale effect. Fig. 6 gives the numerical results of the deflections (v/h) of the beam compared with the exact solutions, which shows that the deflection of the beam in couple stress theory is smaller than that in the classical elasticity ($l = 0$) as the material constant l increased. The numerical results also indicate that the strong size effects appear when the material constant l increased, and the proposed quasi-conforming element can simulate the process.

Fig. 7 shows the maximum errors of tip deflections(v/h) for various ratios l/h by the quasi-conforming element with increasing mesh refinement. The tip deflections v/h and error's percents with mesh refinement is given in Table 4. It is clear that the quasi-conforming element has good accuracy in solving the pure bending beam problem.

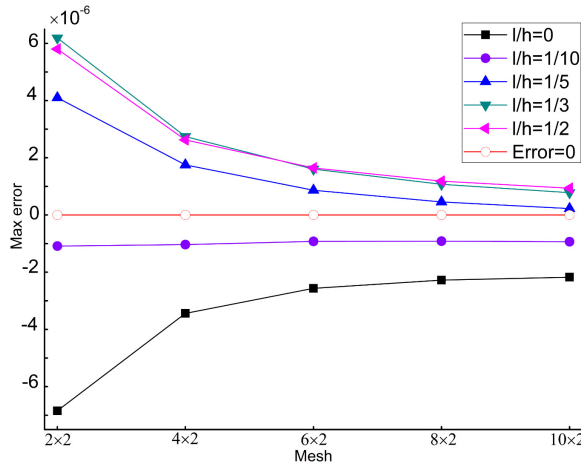


Figure 7: The maximum errors for the pure bending for various ratios l/h with increasing mesh refinement.

Table 4: The tip deflections $(v/h)(10^{-3})$ and error's percents (%) with mesh refinement.

l/h	0.0	1/10	1/5	1/3	1/2
2×2	-3.16228 (0.27)	-2.70822 (0.04)	-1.89402 (-0.22)	-1.10488 (-0.56)	-0.60809 (-0.95)
4×2	-3.15887 (0.11)	-2.70817 (0.04)	-1.89637 (-0.09)	-1.10833 (-0.25)	-0.61127 (-0.43)
6×2	-3.15800 (0.08)	-2.70805 (0.03)	-1.89725 (-0.05)	-1.10946 (-0.14)	-0.61225 (-0.27)
8×2	-3.15771 (0.07)	-2.70805 (0.03)	-1.89766 (-0.02)	-1.10999 (-0.10)	-0.61271 (-0.19)
10×2	-3.15761 (0.07)	-2.70806 (0.03)	-1.89789 (-0.01)	-1.11029 (-0.07)	-0.61296 (-0.15)
Exact	-3.15543	-2.70713	-1.89812	-1.11107	-0.61390

4.4 Simple shear problem

As shown in Fig. 8, a simple shear problem is solved in this section. Due to its simplicity, this problem has recently been studied analytically or computationally as a benchmark problem [Park and Gao (2008)]. The width of the block is w , length

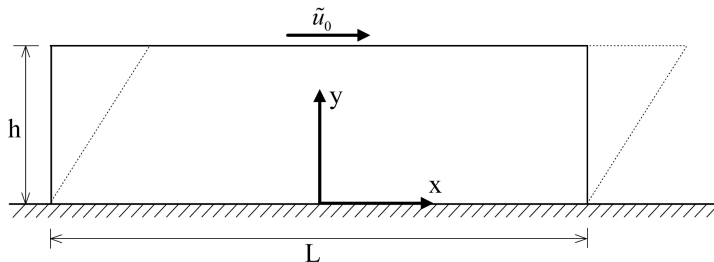


Figure 8: Simple shear problem.

L , height h which undergoing a simple shear deformation. Assumed L and w that are much larger than h such that they both can be viewed as infinite. The prescribed displacement \tilde{u}_0 is induced by a shear force acting on the top boundary $y = h$.

The analysis results with quasi-conforming element are shown in Fig. 9 and Fig. 10, together with the classical elasticity solution [Park and Gao (2008)] for comparison. The material properties for the block are taken to be $E = 1.44\text{GPa}$, $\mu = 0.38$, and four different values of the material constant $l = \{0, 1.76, 8.8, 17.6\}\mu\text{m}$ are

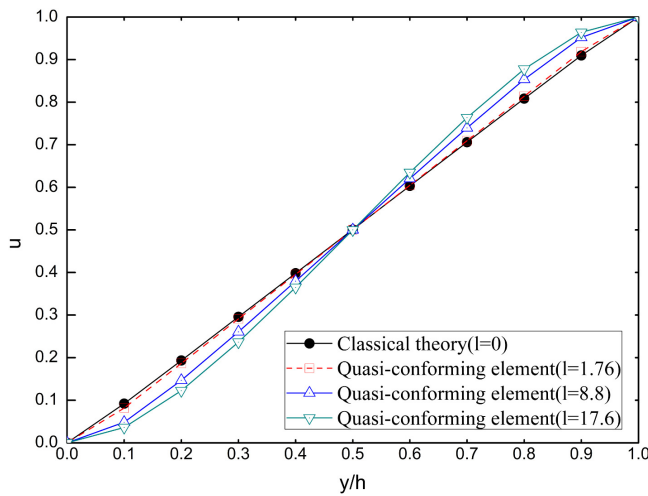


Figure 9: Displacement in the block.

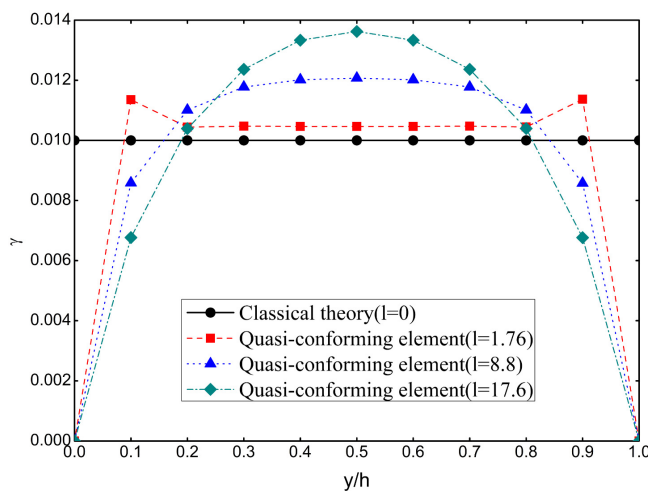


Figure 10: Shear strain in the block.

chosen. The geometric parameters used here are $h = 100\mu\text{m}$, $\tilde{u}_0 = 1\mu\text{m}$.

As shown in Fig. 9 and Fig. 10, the boundary layer effect is captured by the present solution. Moreover, the compared results demonstrate that the influence of the microstructure (though l) can be significant: the larger the value of l , the larger the difference between the present solution and the classical elasticity solution. The numerical results quantitatively indicate that the influence of the length scale parameter is significant.

5 Conclusions

In this paper, we propose a quasi-conforming formulation method, which is perfectly suitable for establishing couple stress element. Strain and strain gradient are approximated by using polynomial function matrices, and appropriate interpolation functions are chosen to calculate strain integration. The element is used for numerical analysis on C^{0-1} patch test, eigenvalue test, pure bending problem and simple shear problem. Numerical results demonstrate that the proposed model can pass the C^{0-1} enhanced patch test and has high accuracy, and the element does not exhibit extra zero energy modes and can capture the scale effects of microstructure.

Acknowledgement: The project was supported by the Fundamental Research Funds for the Central Universities (DUT14RC(3)092), the National Natural Science Foundation of China (No. 11272075, 11472071).

Appendix A: The formulations of Green's theorem

$$\begin{aligned} \iint \frac{\partial^2 u}{\partial^2 x} dx dy &= \oint n_x^2 \frac{\partial u}{\partial n} ds - \sum_i (n_x n_y)_i (u_{i+1} - u_i) \\ \iint \frac{\partial^2 u}{\partial^2 x} x dx dy &= \oint n_x^2 \frac{\partial u}{\partial n} x ds + \oint u (n_x n_y \frac{\partial x}{\partial s} - n_x) ds - \sum_i (n_x n_y)_i ((ux)_{i+1} - (ux)_i) \\ \iint \frac{\partial^2 u}{\partial^2 x} y dx dy &= \oint n_x^2 \frac{\partial u}{\partial n} y ds + \oint u n_x n_y \frac{\partial y}{\partial s} ds - \sum_i (n_x n_y)_i (u_{i+1} y_{i+1} - u_i y_i) \end{aligned} \quad (38)$$

$$\begin{aligned} \iint \frac{\partial^2 u}{\partial^2 y} dx dy &= \oint (n_y)^2 \frac{\partial u}{\partial n} ds + \sum_i (n_x n_y)_i (u_{i+1} - u_i) \\ \iint \frac{\partial^2 u}{\partial^2 y} x dx dy &= \oint (n_y)^2 \frac{\partial u}{\partial n} x ds + \sum_i (n_x n_y)_i ((ux)_{i+1} - (ux)_i) - \oint n_x n_y u \frac{\partial x}{\partial s} ds \\ \iint \frac{\partial^2 u}{\partial^2 y} y dx dy &= \oint (n_y)^2 \frac{\partial u}{\partial n} y ds + \sum_i (n_x n_y)_i ((uy)_{i+1} - (uy)_i) - \oint u (n_x n_y \frac{\partial y}{\partial s} + n_y) ds \end{aligned} \quad (39)$$

$$\begin{aligned}
\iint \frac{\partial^2 u}{\partial x \partial y} dx dy &= \oint n_x n_y \frac{\partial u}{\partial n} ds + \sum_i (n_x)_i^2 (u_{i+1} - u_i) \\
\iint \frac{\partial^2 u}{\partial x \partial y} x dx dy &= \oint n_x n_y \frac{\partial u}{\partial n} x ds - \sum_i (n_y)_i^2 ((ux)_{i+1} - (ux)_i) + \oint n_y^2 u \frac{\partial x}{\partial s} ds \\
\iint \frac{\partial^2 u}{\partial x \partial y} y dx dy &= \oint n_x n_y \frac{\partial u}{\partial n} y ds + \sum_i (n_x)_i^2 ((uy)_{i+1} - (uy)_i) - \oint n_x^2 u \frac{\partial y}{\partial s} ds \quad (40)
\end{aligned}$$

References

- Aifantis, E.** (1984): On the microstructural origin of certain inelastic models. *Journal of Engineering Materials and Technology*, vol. 106, no. 4, pp. 326–330.
- Altan, S.; Aifantis, E.** (1992): On the structure of the mode III crack-tip in gradient elasticity. *Scripta Metallurgica et Materialia*, vol. 26, no. 2, pp. 319–324.
- Bažant, Z. P.** (2002): Concrete fracture models: testing and practice. *Engineering Fracture Mechanics*, vol. 69, no. 2, pp. 165–205.
- Bažant, Z. P.; Pang, S.-D.** (2007): Activation energy based extreme value statistics and size effect in brittle and quasibrittle fracture. *Journal of the Mechanics and Physics of Solids*, vol. 55, no. 1, pp. 91–131.
- Chen, J.; Li, C.** (2014): A quadrilateral spline element for couple stress/strain gradient elasticity. *Computers & Structures*, vol. 138, pp. 133–141.
- Cosserat, E.; Cosserat, F.** (1909): Théorie des corps déformables. *Paris: Hermann et Fils*;
- Dong, L.; El-Gizawy, A.; Juhany, K.; Atluri, S.** (2014): A simple locking-alleviated 3d 8-node mixed-collocation c 0 finite element with over-integration, for functionally-graded and laminated thick-section plates and shells, with & without z-pins. *CMC: Computers Materials and Continua*, vol. 41, no. 3, pp. 163–192.
- Dong, L.; El-Gizawy, A.; Juhany, K.; Atluri, S.** (2014): A simple locking-alleviated 4-node mixed-collocation finite element with over-integration, for homogeneous or functionally-graded or thick-section laminated composite beams. *CMC: Computers, Materials & Continua*, vol. 40, no. 1, pp. 49–77.
- Fleck, N.; Hutchinson, J.** (1993): A phenomenological theory for strain gradient effects in plasticity. *Journal of the Mechanics and Physics of Solids*, vol. 41, no. 12, pp. 1825–1857.

Fleck, N.; Hutchinson, J. (1997): Strain gradient plasticity. *Advances in Applied Mechanics*, vol. 33, pp. 296–361.

Fleck, N.; Muller, G.; Ashby, M.; Hutchinson, J. (1994): Strain gradient plasticity: theory and experiment. *Acta Metallurgica et Materialia*, vol. 42, no. 2, pp. 475–487.

Hu, P.; Xia, Y. (2012): Survey of quasi-conforming finite element method(in Chinese). *Advances in Mechanics*, vol. 42, no. 6, pp. 755–770.

Hu, P.; Xia, Y.; Tang, L. (2011): A four-node Reissner-Mindlin shell with assumed displacement quasi-conforming method. *CMES: Computer Modeling in Engineering and Sciences*, vol. 73, no. 2, pp. 103–136.

Ji, B.; Chen, W. (2010): A new analytical solution of pure bending beam in couple stress elasto-plasticity: theory and applications. *International Journal of Solids and Structures*, vol. 47, no. 6, pp. 779–785.

Koiter, W. (1964): Couple-stresses in the theory of elasticity, I & II. *Proc. K Ned Akad Wet(B)*, vol. 67, pp. 17–44.

Liu, Y.; Shi, G.; Tang, L. (1983): Discussion on the superfluous zero energy modes of finite elements (in chinese). *Journal of Dalian Institute of Technology*, vol. 22, no. 3, pp. 62–67.

Lomboy, G.; Suthasupradit, S.; Kim, K.; Oñate, E. (2009): Nonlinear formulations of a four-node quasi-conforming shell element. *Archives of Computational Methods in Engineering*, vol. 16, pp. 189–250.

Mindlin, R. (1964): Micro-structure in linear elasticity. *Archive for Rational Mechanics and Analysis*, vol. 16, no. 1, pp. 51–78.

Nix, W.; Gao, H. (1998): Indentation size effects in crystalline materials: a law for strain gradient plasticity. *Journal of the Mechanics and Physics of Solids*, vol. 46, no. 3, pp. 411–425.

Papanicolopoulos, S.-A.; Zervos, A.; Vardoulakis, I. (2009): A three-dimensional C^1 finite element for gradient elasticity. *International Journal for Numerical Methods in Engineering*, vol. 77, no. 10, pp. 1396–1415.

Park, S.; Gao, X.-L. (2008): Variational formulation of a modified couple stress theory and its application to a simple shear problem. *Zeitschrift für angewandte Mathematik und Physik*, vol. 59, no. 5, pp. 904–917.

Pian, T. H. (1964): Derivation of element stiffness matrices by assumed stress distributions. *AIAA journal*, vol. 2, no. 7, pp. 1333–1336.

Shi, Z.; Wang, M. (2013): *Finite element methods*. Beijing: Science Press.

Soh, A.-K.; Chen, W. (2004): Finite element formulations of strain gradient theory for microstructures and the C^{0-1} patch test. *International Journal for Numerical Methods in Engineering*, vol. 61, no. 3, pp. 433–454.

Stölken, J.; Evans, A. (1998): A microbend test method for measuring the plasticity length scale. *Acta Materialia*, vol. 46, no. 14, pp. 5109–5115.

Tang, L.; Chen, W.; Liu, Y. (1980): Quasi-conforming elements for finite element analysis (in Chinese). *Journal of Dalian Institute of Technology*, vol. 2, pp. 17–35.

Toupin, R. (1962): Elastic materials with couple-stresses. *Archive for Rational Mechanics and Analysis*, vol. 11, no. 1, pp. 385–414.

Wang, C.; Hu, P. (2012): Quasi-conforming triangular Reissner-Mindlin shell elements by using Timoshenko's beam function. *Computer Modeling in Engineering & Sciences(CMES)*, vol. 88, no. 5, pp. 325–350.

Wang, C.; Hu, P.; Xia, Y. (2012): A 4-node quasi-conforming Reissner-Mindlin shell element by using Timoshenko's beam function. *Finite Elements in Analysis and Design*, vol. 61, pp. 12 – 22.

Wei, Y.; Wang, X.; Wu, X. (2000): Theoretical and experimental study on micro-indentation size effects(in Chinese). *Sci China (A)*, vol. 30, pp. 1025–1032.

Yang, F.; Chong, A.; Lam, D.; Tong, P. (2002): Couple stress based strain gradient theory for elasticity. *International Journal of Solids and Structures*, vol. 39, no. 10, pp. 2731–2743.

Zervos, A.; Papanastasiou, P.; Vardoulakis, I. (2001): Modelling of localisation and scale effect in thick-walled cylinders with gradient elastoplasticity. *International Journal of Solids and Structures*, vol. 38, no. 30, pp. 5081–5095.

Zervos, A.; Papanicolopoulos, S.-A.; Vardoulakis, I. (2009): Two finite-element discretizations for gradient elasticity. *Journal of Engineering Mechanics*, pp. 203–213.

Zhao, J.; Chen, W.; Lo, S. (2011): A refined nonconforming quadrilateral element for couple stress/strain gradient elasticity. *International Journal for Numerical Methods in Engineering*, vol. 85, no. 3, pp. 269–288.